ACETYLCHOLINESTERASE IN THE FAST EXTRAOCULAR MUSCLE OF THE MOUSE BY LIGHT AND ELECTRON MICROSCOPE AUTORADIOGRAPHY

MIRIAM M. SALPETER, ANDREW W. ROGERS, HEDWIG KASPRZAK, and FRANCES A. McHENRY

From the Section of Neurobiology and Behavior and the School of Applied and Engineering Physics, Cornell University, Ithaca, New York 14853. Dr. Rogers' present address is Human Morphology Unit, Flinders Medical School, Bedford Park, South Australia 5042.

ABSTRACT

The distribution of acetylcholinesterase (ACh) in the twitch fibers of the extraocular muscles of the mouse was examined by light and electron microscope autoradiography after labeling with radioactive diisopropyl fluorophosphate (DFP) with, and without, 2-pyridine aldoxime methiodide (2-PAM) reactivation. The values obtained were compared with those previously reported for the diaphragm and sternomastoid muscles. The extraocular muscles were studied because they differ from the other two muscles in that they are among the fastest of the mammalian muscles, yet their endplates have sparse junctional folds. They could thus provide information on the extent to which ACh concentration is an invariant feature of endplate morphology and what, if any, aspects may be related to their fast speed of response.

We found, using light microscope autoradiography, that in the twitch fibers of the extraocular muscle, there is an average of $6.4 \pm 2.1 \times 10^7$ DFP-binding sites per endplate, of which 29% (1.8×10^7) are reactivated by 2-PAM and are thus ACh. The morphology of the extraocular endplates allowed us to conclude, on statistical grounds, that the ACh sites are probably localized not only along the surface area of the postjunctional membrane (PJM) but also along the surface of the presynaptic axonal membrane. Based on this localization, we calculate 7,800 DFP sites and 2,500 2-PAM-reactivated sites/μm^2 of surface area of pre- and postjunctional membrane. This stacking density of DFP-binding sites per surface area of membrane (probably in the overlying sheets of basal lamina) is very similar to that in the diaphragm and sternomastoid muscles.

KEY WORDS acetylcholinesterase · extraocular muscle · EM autoradiography · track autoradiography · neuromuscular junctions · acetylcholine receptor

In several studies we have assessed the number of esterase sites both at the whole endplate (31, 32) and on the fine structural level (33, 34, 41). We found that in two different mouse muscles, the diaphragm and sternomastoid, there were about the same number of labeled sites per square micrometer of the folded postjunctional membrane (PJM). These data suggested that the esterases may be present in muscles in some constant

 J. CELL BIOLOGY © The Rockefeller University Press · 0021-9525/78/0701-0274$1.00

relationship to the PJM, independently of muscle morphology or speed of response (4). However, although mouse diaphragm and sternomastoid muscles differ somewhat both in morphology and speed of response (e.g., the diaphragm consists primarily of red fibers and has a fusion frequency for maximum tetanic contraction of 25–30 Hz whereas the sternomastoid consists primarily of white fibers and has a tetanic fusion frequency of 70–80 Hz), the overall differences are not very great, and in both muscles there is a similar ratio (5–6:1) of postjunctional to prejunctional membrane. It was, therefore, difficult to draw any firm conclusions concerning the above hypothesis based on data from these two muscles alone.

A muscle which is ideally suited for testing the hypotheses that the esterase site density remains a constant function of junctional-fold surface area is the extraocular muscle, because in this muscle the junctional folds are relatively sparse when compared with the other two mouse endplates studied (40), i.e., the ratio of postjunctional to presynaptic axonal membrane is 2–3:1. Thus, a constant ratio of acetylcholinesterase (ACh) to PJM surface area would leave this muscle with relatively less ACh than is present in the other two muscles. Yet the extraocular muscle is among the fastest of the mammalian twitch muscles, having tetanic fusion frequencies 5–10 times faster than those of the other two muscles (350–450 Hz) (1, 8, 10, 20), and thus it may be expected to have a greater need for ACh to allow for rapid repetitive action. The unique morphology of the extraocular muscle allowed us to determine the extent to which ACh concentration is indeed a constant function of junctional fold membranes.

The endplates were labeled using diisopropyl fluorophosphate (DFP), which phosphorylates the active sites of a number of esterases and proteases by forming a covalent bond with a serine residue (see discussion by Cohen et al. [9]). The reaction kinetics and subsequent fate of the phosphorylated enzymes depend on species and class of enzymes, as well as on pH and temperature. Studies on mammalian esterases which have been phosphorylated with DFP indicate that this reaction is essentially irreversible but that the enzyme can be quickly reactivated by certain nucleophilic reagents. One such agent, 2-pyridine aldoxime methiodide (2-PAM), is among the most potent specific reactivators for phosphorylated ACh (44, 45). Thus, by labeling the 2-PAM-reactivated sites, one can distinguish ACh from other DFP-phosphorylated sites. In our earlier studies (30), the validity of the use of 2-PAM reactivation was established by showing that the same fraction of sites was protected from DFP by the specific ACh inhibitor BW 284C51.

In the present study on the extraocular muscles, we first used light microscope autoradiography to determine both the total number of DFP-binding sites per whole endplate and the number of these sites reactivated by 2-PAM. EM autoradiography was then used to study the subcellular distribution of these sites. The sizes of the endplate compartments were also determined, as previously described (38).

MATERIALS AND METHODS

The four rectus muscles of the eye in adult albino mice were used. They were labeled either by: (*a*) radioactive DFP, to phosphorylate all reactive sites; (*b*) radioactive DFP followed by 2-PAM, to label all reactive sites except ACh; and (*c*) nonradioactive DFP, followed by 2-PAM and then by radioactive DFP to label ACh sites only. Conditions for saturation of DFP sites, for minimizing nonspecific binding, and for reactivating with 2-PAM have previously been established and were followed here (31, 32). Saturation with DFP was always judged by the absence of cholinesterase reaction products after a 1/2-h staining period using the method of Karnovsky and Roots (24). The conditions were also designed to eliminate any significant effect of "ageing" on the quantitative results by keeping the time lapse between the DFP and the 2-PAM incubation to <1 h. ("Ageing" is a process whereby dealkylation of the organophosphorous inhibited enzymes occurs with time and prevents reactivation by 2-PAM. The accumulated evidence from several studies [5, 9, 11, 14, 21, 22, 23] leads to the conclusion that the half-life for ageing of ACh inactivated with DFP is longer than for butyrylcholinesterase (BuCh), is on the order of 10–35 h at room temperature, and is temperature-dependent.)

Light Microscope Autoradiography

TRACK AUTORADIOGRAPHY: Light microscope track autoradiography was used to obtain the total DFP-binding sites per whole endplate. Two male Swiss mice, each weighing ~16 g, were killed by a blow on the head. The rectus muscles from each eye were fixed in cold 4% formalin in phosphate buffer (pH 7.4) and stained for ACh by the method of Karnovsky and Roots (24). This stain was used instead of a Koelle stain previously used by Rogers et al. (32) since the latter caused a progressive reduction with time of the sites available for reaction with DFP. After staining, the muscles were washed in phosphate buffer, then incubated with [^{32}P]DFP (Radiochemical Centre, Amersham, England; sp act 0.2 mCi/0.66 mg of DFP), and finally washed in nonradioactive

DFP and in buffer, as previously described (31, 32). The muscles were teased into individual muscle fibers. The regions bearing stained endplates were then microdissected, placed on gelatinized slides, and coated with a thick (60–100 μm) layer of Ilford G5 emulsion (Ilford Ltd., Ilford, Essex, England). The preparations, after drying, were exposed for 23.5 h. The emulsion was processed in an Amidol developer and prepared for track counting (30).

Tracks were counted using a KS × 53 objective on a Leitz Ortholux microscope. Only tracks traveling upwards into the emulsion from the muscle fibers were counted and were assumed to represent 50% of the total number of β-particles leaving the fibers during exposure (the remainder traveling down into the glass slide). Background values obtained from similar lengths of the same fiber at a position distant from the endplate were then subtracted.

GRAIN DENSITY AUTORADIOGRAPHY: Light microscope grain density autoradiography was used as a means of determining the fraction of all DFP sites that is reactivated by 2-PAM and thus is AChe. The rectus muscles were again dissected from two male mice and fixed as for track autoradiography, but were then incubated in 10^{-4} M [^{3}H]DFP (Radiochemical Centre; sp act 4.3 Ci/mmol), rather than in [^{32}P]DFP. The muscles were washed in nonradioactive DFP and in buffer as was done for the [^{32}P]DFP-treated muscle. They were then divided into two groups, A and B. Group A was incubated in [^{3}H]DFP as described above. Group B was further treated with 2-PAM (10^{-3} M, pH 7.8, for 40 min at room temperature) to remove the [^{3}H]DFP specifically from AChe sites and thus provide tissue in which *all but* AChe sites were labeled. The muscles were then washed and sectioned on a cryostat at −24°C at a thickness of 5μm. The sections were mounted on gelatinized slides, which were then dipped in Ilford L4 emulsion, exposed for 12 days, and processed in an Amidol developer, as were the track autoradiograms.

To recognize endplates for grain counting, all slides were stained through the developed emulsion by the technique of Karnovsky and Roots (24). Specimens for group A (i.e., in which all sites had been phosphorylated) were first incubated in a solution of 10^{-2} M 2-PAM for 30 min to reactivate phosphorylated sites, thus permitting AChe staining. Since this 2-PAM treatment of group A autoradiograms was done after the photographic processing was complete, the autoradiographic results were not affected. (Autoradiograms of group B were not treated with 2-PAM after photographic processing since the AChe was already reactivated as part of the initial incubation sequence.)

All grain counting was carried out by the same observer. Stained endplates were identified on the sections and their areas measured using a calibrated grid in the ocular (unit area = 30 μm^2). Background correction was based on the grain counts over similar areas of muscle fiber without endplate.

Statistically, one can expect the fraction of an endplate which will be seen by the emulsion to be roughly the same for groups A and B. The difference between the grain counts in the two groups can therefore be used to determine the fraction of sites reactivated by 2-PAM.

EM Autoradiography

The four lateral rectus muscles of six animals were used. The muscles were either fixed in vitro by immersion in 1.5% glutaraldehyde in 0.06 M phosphate buffer, pH 7.4 (2 h on ice as previously done [34, 41]), or by perfusion of the whole animal in the periodate lysine-paraformaldehyde fixative (2% in 0.06 M phosphate with 6.8% sucrose) (27), followed by 2-h immersion fixation in the same fixatives. In a recent study,[1] it was found that the DFP-binding-site density is not significantly different with these two fixation procedures.

Tissue regions rich in endplates were used. They were thoroughly washed in cold phosphate buffer with 6.8% sucrose, and then incubated either (*a*) in [^{3}H]DFP, to label all DFP sites, or (*b*) with the sequence nonradioactive DFP → 2-PAM → [^{3}H]DFP, to label only 2-PAM-reactivated sites. The incubation procedures were as previously described (33, 34, 41); DFP incubation was performed at pH 7.4 and 2-PAM incubation at pH 7.8, both in 0.06 M phosphate buffer. The tissues were then postfixed in 1% OsO_4 in 0.06 M phosphate buffer, block stained in 2% aqueous uranyl nitrate or acetate, and embedded in Epon 812.

Absolute quantitation was made possible by the use of the "flat substrate" EM autoradiography method of Salpeter and Bachmann (35, 36). For each animal, pale gold sections were cut from six different regions of the muscle (i.e., two different regions of three blocks or three different regions of two blocks) to get adequate sampling. The sections were coated with a tightly packed monolayer of Ilford L4 emulsion (deep purple interference color), exposed for ~15 wk and developed either with Microdol X (Eastman Kodak Co.) for 3 min or with Gold latensification (GEAS) (43). Autoradiograms were systematically scanned in the EM and all endplates photographed, regardless of whether there were any grains associated with them or not. At least 200 endplate profiles per animal were tabulated, representing a broad sampling from all the muscles processed. The micrographs were enlarged photographically to a final magnification of 20,000–30,000 for grain tabulation.

Analysis of Autoradiograms

The grain density distribution method (37, 39) was used on endplates of two animals to establish the localization of radioactivity in the subneural region of the endplate. This procedure was used in our previous studies on DFP binding to other mouse endplates (34,

[1] Kasprzak, H., and M. Salpeter. Manuscript in preparation.

41) and consists of comparing experimentally obtained grain distributions around assumed sources with what one would expect from such sources based on the resolution of the technique used. The "goodness of fit" between the expected and experimentally obtained distributions allows one to define the likely sources of radioactivity in the tissue. Once this was done, all animals were analyzed for absolute quantitation. Grain density (grains per unit area or volume of each potential source) was tabulated, and the absolute site density calculated as previously described[2] (34, 37, 41).

RESULTS

Morphology of Endplates in Extraocular Muscle

The fine structure of the myoneural junctions of mouse extraocular muscle was described in a previous study (40). There are two major categories of myoneural junctions: multiple junctions on tonic fibers and single junctions on twitch fibers. The single junctions were tentatively further subdivided into two groups. The first group (60–70% of total) consists of large diffuse endings seen on thin, mitochondrion-rich ("dark red") fibers (Fig. 1*a*). These endings have very sparse junctional folds (Figs. 1*b* and 3). The second group consists of smaller (more compact) junctions on larger fibers with many fewer mitochondria ("off-white" fibers). (For further illustrations, see reference 40.) These endings have somewhat more extensive junctional folds. The overall average ratio of PJM to presynaptic axonal membrane of both types of endplates in both the earlier and the present study is 3:1. (In many of the endplates on the dark red fibers, the ratio is as low as 1.5:1 and on off-white fibers as high as 5.5:1.) The depth of the folds is 0.3 μm. These ratios of membrane lengths and depth-of-fold averages were based on measurements made on numerous random sections through the endplates of several different animals and were found to vary within ± 30% of these mean values. It is not always easy to distinguish between the two types of endplates on the extraocular twitch fibers, and a continuum in the morphology of both the endplates and their muscle fibers is a real possibility (40). In the present study, the problem of subdividing the single endplates on twitch fibers was especially great for the light microscope images, so in the specimens for light autoradiography no clear distinction between the diffuse and compact single endplates was made. In the EM, these were more easily distinguished. Since the diffuse single endplate on the "dark red fiber" is the prevailing endplate in the extraocular muscle, the statistical analysis reflects predominately their input. However, in two animals we analyzed small subsamples of endplates on off-white fibers separately and did not note any significant difference in the distribution of their DFP-binding-site density.[3]

Light Microscope Autoradiography, Track, and Grain Density

From track autoradiography we obtained information on DFP binding sites per whole endplate. We identified 44 single endplates and 202 β-tracks (after background subtractions) originating from them in the direction toward the emulsion. From the specific activity of the DFP and the sensitivity of the calibrated technique, we could determine that this is equivalent to $6.4 \pm 2.1 \times 10^7$ DFP-binding sites per endplate. There was a large variation in endplate sizes, the surface area ranging from ~1,000 to 6,000 μm^2. The large standard deviation in binding sites partly reflects an increased number of tracks with increased endplate size. (Surface area was judged by the overall extent of the reaction product in surface view after staining for AChe.) However, as can be

[2] The sensitivity value was obtained from the sensitivity curves reported by Salpeter and Szabo (43). The grain density over the cleft was used to read the appropriate sensitivity value which, in the present study, was 1/10–1/12 for most of our autoradiograms developed with Microdol X. Because of the high "dose dependence" with Microdol X, which introduces a systematic error and can limit the accuracy of the absolute quantitation by ~30%, we no longer recommend the use of the Microdol X developer. The study reported here, however, was begun before this dose dependence was discovered. At that time we began using Gold EAS or D19 developers which gave sensitivity values of 1/4–1/5.

[3] The small multiple endings on the tonic fibers were not easily detectable by the light microscope autoradiographic techniques. Only five multiple endings were seen in the track autoradiography. These had in total only two β-tracks above background and thus were essentially below the sensitivity of the light autoradiographic procedures used. In the EM study, we had no problem seeing the multiple endings on the tonic fibers but found an insufficient number of developed grains associated with them for a statistical analysis. The current study was thus restricted to the single endplates on twitch fibers.

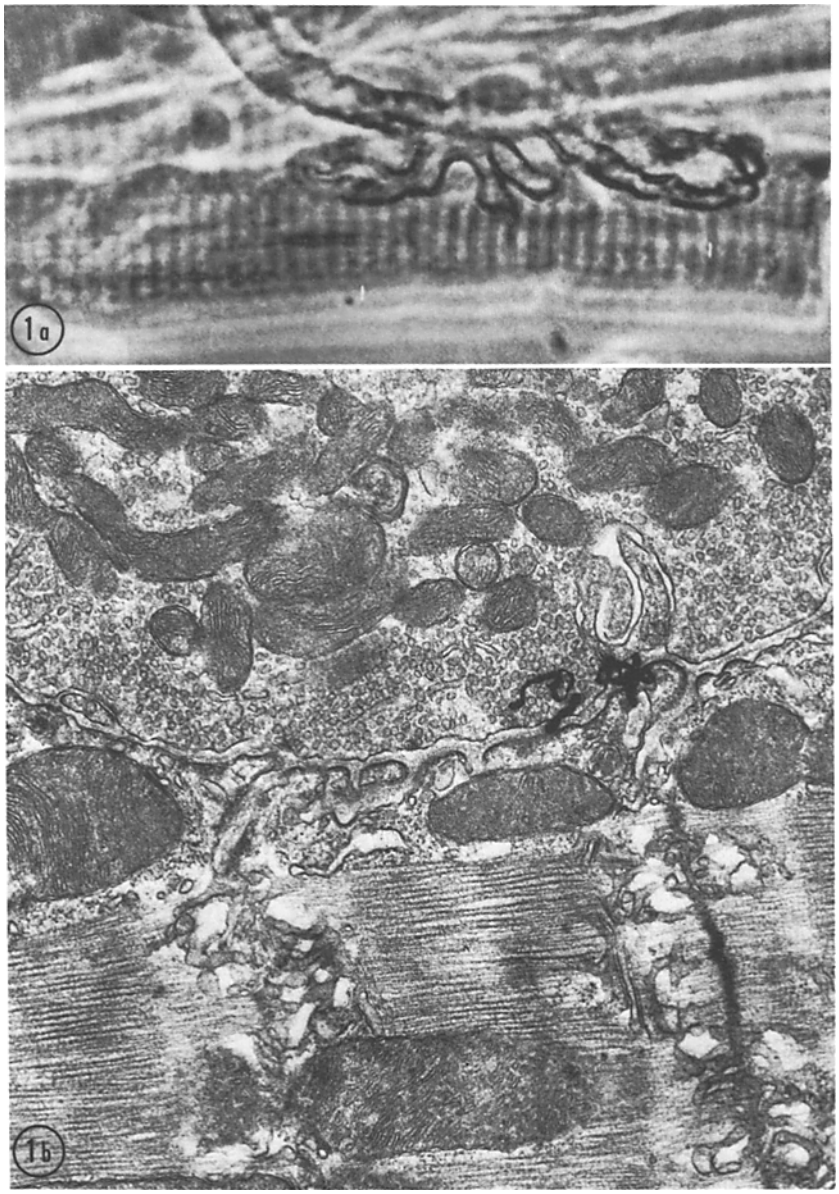

FIGURE 1 (*a*) Large diffuse endplate on teased extraocular dark red fiber stained for AChe and seen by phase microscopy. × 1,000. (*b*) EM autoradiograph of extraocular endplate on a dark red twitch fiber as illustrated in Fig. 1 *a*. Note sparse junctional folds. × 20,200.

seen from Fig. 1 *a*, the axonal terminal branches fan out in a diffuse manner and the overall surface area of the endplate is not strictly related to functional area of the endplate. No exact correlation between overall size of endplate and autoradiography tracks could therefore be established.

The light microscope grain density autoradiography (after [^{3}H]DFP binding with and without 2-PAM) was used for assessing the percent of sites reactivated by 2-PAM since it was deemed more accurate than the track autoradiography for this purpose. This is because a large sample is more easily obtained and the area for tabulating developed grains is well-defined and restricted to portions of the endplate which are functionally related to esterase activity. The section and emulsion

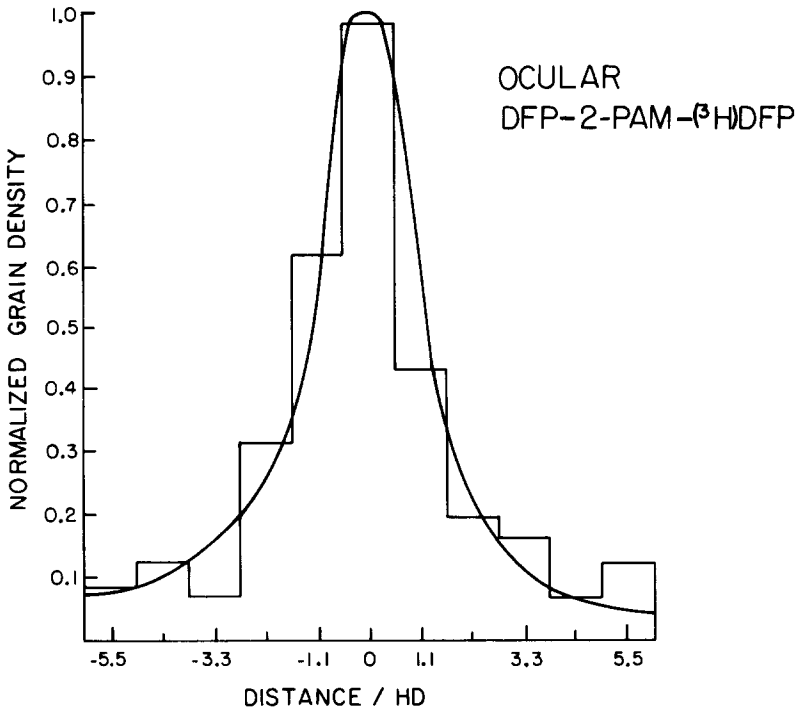

FIGURE 2 Histogram of grain density centered on postjunctional folded membranes. Distances measured in resolution units, HD (37).

thicknesses are infinite for tritium radiation and thus small fluctuations in specimen thickness do not contribute to the autoradiographic variance. However, the grain density light microscope autoradiograms are not suitable for absolute quantitation of sites per whole endplate because of the difficulties in determining the fraction of the whole endplate which is included in the tabulation.

Thus, in group A (i.e., all DFP-binding sites) 132 endplates on twitch fibers were recognized in sections and their areas measured. In the overlying emulsion, 493 grains were counted, giving a grain density of 16.96 grains/100 μm^2 of endplate area. In group B (all DFP sites minus 2-PAM-reactivated sites, i.e., 2-PAM insensitive sites), 204 sectioned endplates were identified and measured, and 933 grains, or 12.11 grains/100 μm^2 were found. Therefore, by comparing groups A and B, it was determined that 28.6% of the DFP-reactive sites are AChe.

If the results from track and grain density light microscope autoradiography are combined, we conclude that in this heterogeneous population of singly innervated fibers there is an average of 6.4 $\times$ 10^7 DFP-binding sites per whole endplate, of which an average of 28.6% are reactivated by 2-PAM. This gives a value of 1.8 $\times$ 10^7 AChe sites per endplate.[4]

EM Autoradiography

GRAIN DENSITY HISTOGRAM: Fig. 1*a* shows a stained endplate on a "dark red" fiber in surface view, and Fig. 1*b* an EM autoradiograph of a typical profile through such an endplate. Fig. 2 gives a grain density histogram of AChe sites based on 433 grains from 184 endplates of two animals and constructed around the postjunctional membrane as previously described (34, 41). The smooth curve superimposed over the experimental

[4] We now think that the values reported previously for the eye muscles by Barnard and Rogers (3) are in error. These authors reported two experiments in which ocular muscles were examined. In the first, 36 endplates gave a value of 5–6 $\times$ 10^7 DFP-reactive sites per endplate; in the second, 21 endplates, observed to be much smaller, gave 1.25 $\times$ 10^7 DFP-reactive sites per endplate. It was assumed that the second experiment had involved tonic endplates; the first, twitch. On reexamination of the original slides, it is clear that the smaller, second group did not consist of tonic endplates, but rather were small twitch endplates, compatible with the lower end of the size range seen in the present experiments.

histogram was derived from Salpeter et al. (37) and represents the expected grain distribution from a line source coincident with the postjunctional folded membrane corrected for the curvature of the axonal endbulb. It was found that, as in the other two mouse muscles, the experimental data are compatible with the hypothesis that the radioactive source is centered within one resolution width (HD) of the postjunctional folded membrane. (The parameter, HD, was defined in studies on EM autoradiographic resolution as that distance from a line source within which 50% of the grains due to that source would fall.) For the autoradiographic conditions used here, HD is 1,500 Å (37). Since the one-HD distance from the postjunctional membrane included the synaptic cleft as well as the presynaptic axonal membrane, these two structures cannot be resolved directly from the postjunctional membrane by the procedure used in this analysis and therefore cannot be excluded as possible sources of radioactivity.

We therefore had three potential sources, i.e., the cleft, the postjunctional folded membrane (PJM) alone, and the combined prejunctional plus PJM (prejunctional membrane is defined as that part of the axonal membrane which is adjacent to the postjunctional membrane, i.e., bounding the primary cleft). Site densities were first determined for these three endplate compartments as if each was the true source. All the grains within the histogram distances in Fig. 2 were used to calculate the concentration of sites relative to the three compartments. Background grains seen over an equivalent area away from the endplate were subtracted. The number of DFP- or 2-PAM-reactivated sites per unit surface area or volume was then calculated (as previously described in references 34 and 41). The results are given in Table I.

THE MOST LIKELY SOURCE OF RADIOACTIVITY: The geometry of the extraocular endplates provided an indirect means of estimating the most probable localization of the radioactivity (i.e., the true source compartment). As can be seen in Fig. 1*b*, the predominant endplate (i.e., large diffuse endplate on dark red fibers) in the extraocular muscle has very sparse junctional folds. Also, the amount of folding varies within one endplate, in that there are areas with no folds and other areas with more frequent folds. This variation provided the opportunity for a statistical analysis to help localize the binding sites. The analysis was performed only on the 2-PAM-reactivated sites from two animals. The endplates were subdivided into two zones (Fig. 3). *Zone 1* consisted of regions where there were no postjunctional folds; *Zone 2* consisted of regions containing junctional folds, and included one resolution width (HD 1,500 Å) on either side of the folds. (Any zone segment less than one HD wide was omitted from the tabulation to minimize the effect of cross scatter.) Grain densities related to different endplate compartments were analyzed separately for the two zones.

The expectation was that the number of grains should vary between the two zones to the same extent as the areas or volumes of the "true source" (i.e., the endplate compartment with which the radioactivity is associated). Or, in other words, the grain densities related to that compartment which was the true source should remain constant in the two zones. (The results are seen in Table II). We found by performing χ^2 tests that only when the grains were related to the areas of the

TABLE I

*DFP-Binding-Site Density for Different Assumed Sources at Endplates of Extraocular Muscle**

	Assumed source					
	PJM surface area: sites ($10^3/\mu m^2$)		Axonal plus PJM surface area§ sites ($10^3/\mu m^2$)		Cleft volume: sites ($10^3/\mu m^3$)	
Muscle	total DFP	2-PAM reactivated	total DFP	2-PAM reactivated	total DFP	2-PAM reactivated
Extraocular twitch fiber‡	11.3 (8.2-14.2)	3.4 (2.4-4.2)	7.8 (6.2-9.6)	2.5 (1.9-2.6)	136.7 (122-146)	41.4 (33.7-49.1)
Sternomastoid‖	9.3	2.4	7.8	2.0	123.2	35.2
Diaphragm¶	8.6	2.2	7.2	1.8	130.0	29.0

* Compared with that of other mouse muscles.

‡ Based on six animals and 36 tissue samples; range of values given in parentheses.

§ Most likely true source in extraocular twitch fibers (see Table II). This information is not yet available for sternomastoid and diaphragm muscles.

‖ Data from Salpeter et al. (41), and H. Kasprzak and M. Salpeter, manuscript in preparation.

¶ Data from Salpeter et al. (41).

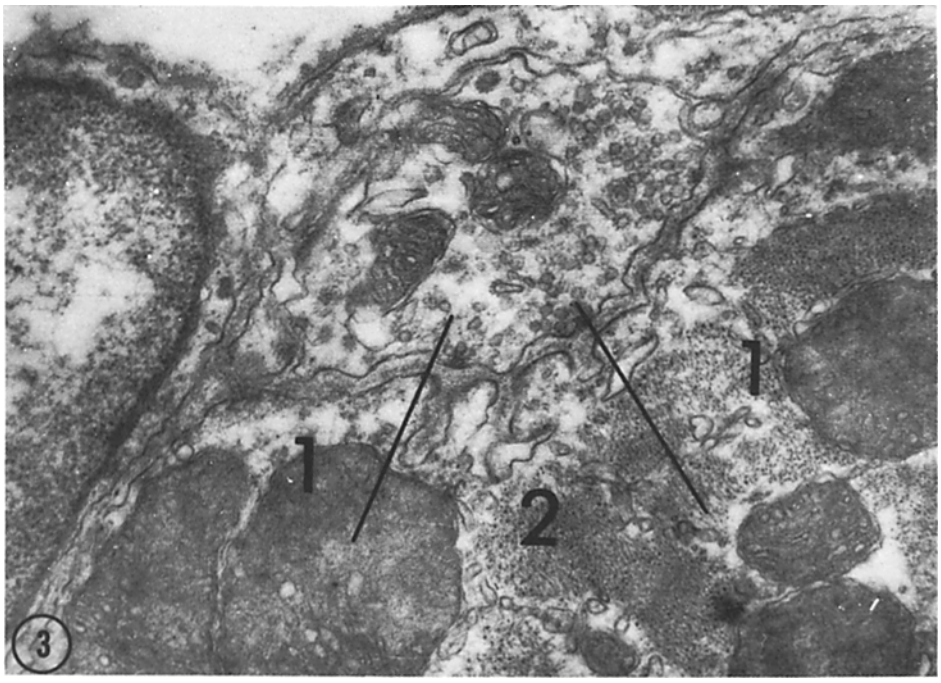

FIGURE 3 Extraocular junction of dark red fiber to illustrate *Zones 1* and *2* representing regions without and with junctional folds, respectively. × 30,680.

TABLE II

*Search for Most Likely Source of Radioactivity in Extraocular Endplates**

Endplate zones‡	Number of grains	Grains/unit area or volume (arbitrary units)§ related to different assumed source compartments		
		PJM surface area¶	Axonal plus PJM surface area‖	Cleft volume¶
Zone 1 (PJM has no folds)	102	1.14	0.59	3.50
Zone 2 (PJM has folds)	107	0.69	0.53	2.48

* The rationale underlying these calculations is the assumption that the true source compartment is, on the average, equally labeled in the entire endplate. Three possible labeled (source) compartments were considered: (*a*) the basal lamina along the surface of the PJM; (*b*) the basal lamina along both the axonal and PJM surface; and (*c*) the entire volume of the cleft. Each of the above was then assumed to be the only source compartment. For each zone, we then calculated separately what the grain density would be if all the grains were due to radioactivity from only that compartment. Since the relative sizes of the three compartments differ in *zones 1* and *2*, only the true source compartment is expected to have the same grain density in each zone. (See footnote ‖ below.)

‡ For illustrations of *zones*, see Fig. 3.

§ When comparing grain density in different zones from the same set of endplates the variance is expected to be merely the sampling error due to the number of grains counted and the measurements of the compartment size. These are estimated to be <15% for the conditions of this analysis.

‖ Most likely the true source. χ^2 for *zones 1* and *2* is not significantly different ($P = 0.5$).

¶ χ^2 is significantly different ($P < .02$) for *zones 1* and *2*.

total junctional membranes (pre- plus postjunctional) were the grain densities not significantly different in the two zones ($P = 0.5$). The grain densities were, however, significantly different ($P = < 0.02$) between *zones 1* and *2* when grains were related either to the postsynaptic membrane areas alone or to the entire volume of the cleft. We conclude from these results that the most likely distribution of the AChe sites is along the surface area of both, the presynaptic axonal and

postjunctional (junctional fold) membranes. Recent studies have provided evidence that the AChe is associated with the basement membrane (basal lamina) of the cleft and not the plasma membrane (6, 7, 19, 28). The basal lamina appears in fine structure as sheets along the surface contours of both the PJM and axonal membrane, although sometimes the two lamina appear fused. In the present study, we use the term "surface area of the axonal or PJM" to include the sheets of basal lamina which lie along these surfaces.

SIZE OF ENDPLATE COMPARTMENTS: One can calculate the absolute sizes of the subneural endplate compartments (i.e., surface area of synaptic membranes and volume of cleft) using the following equation (38):

$$\frac{\text{subneural sites per whole endplate}}{\text{sites per } \mu m^2 (\text{or } \mu m^3) \text{ of compartment}} = \text{size of compartment } (\mu m^2 \text{ or } \mu m^3). \quad (1)$$

About 90% of entire endplate AChe sites is over the subneural compartments, the rest being in the teloglial cap (i.e., Schwann cell and surrounding connective tissue). We therefore used 90% of the sites per whole endplate (from the track autoradiographic data) to get the number of subneural sites per whole endplate for the numerator of the above equation. The site densities per square micrometer of membrane or per cubic micrometer of cleft (from the EM autoradiographic results in Table II) were used for the denominator of the equation. The resultant sizes of the subneural compartments, compared with those of the diaphragm and sternomastoid muscles, are given in Table III.

DISCUSSION

The results of this study indicate that there is an amazing constancy in the AChe site density per unit surface area of the junctional membranes when comparing the very fast extraocular muscle endplate with other mouse endplates varying in relative PJM surface area and in speed of the muscle response (Table I). Also, in terms of total DFP sites ($\sim 6 \times 10^7$) per whole endplate as well as the fraction of these sites that are AChe ($\sim 30\%$), the fast eye muscles are similar to the slower sternomastoid and diaphragm muscles. Many early studies (12, 13, 15, 33, 34, 41) have placed the enzyme over a broad zone extending over the depths of the junctional folds. There is now good evidence that it is associated with the basement lamina of the clefts (6, 7, 19, 29). In the present study, we present a statistical argument (Table II) that at least in the endplates of the singly innervated "dark red" extraocular fibers, the AChe sites are distributed on or along both the axonal and postjunctional membranes, at a uniform density per square micrometer of membrane surface area rather than per cubic micrometer of cleft volume. This conclusion is compatible with the localization of the enzymes within the basal lamina, provided these lamina form sheets along the outer surface of the membranes.

The significance of the conclusion that the enzyme may be distributed along the surface of both the pre- and postjunctional membranes (Table II) needs some consideration. From Table I, we see that with such a distribution, the average site density per square micrometer of membrane surface differs merely by 25% from what it would be

TABLE III

Surface Areas (or Volumes) of Endplate Compartments in Different Mouse Muscles*

Muscle	Endplate compartment		
	Cleft volume	PJM surface	Prejunctional axonal membrane
	μm^3	μm^2	μm^2
Extraocular twitch	400 (400; 400)	4,750 (5,100; 4,400)	1,950 (2,300; 1,600)
Sternomastoid	660 (643; 675)	9,200 (8,500; 9,900)	1,820 (1,650; 1,980)
Diaphragm	260 (207; 310)	3,620 (3,140; 4,091)	800 (610; 990)

* Sizes were obtained from Eq 1 and each value is an average from two independent determinations; the first using total DFP binding sites (first value in parentheses) and the second using 2-PAM-reactivated sites (second value in parentheses). Since the sizes should be independent of the nature of the sites used in the calculation, the difference in the two values reflects merely statistical fluctuation in both the numerator (sites per whole endplate) and the denominator (sites per unit area or volume) of the two determinations. Since each is accurate to $\sim \pm 25\%$ the final value given is estimated to be accurate to better than $\pm 40\%$.

if the enzyme were only along the PJM, even in the extraocular fibers (where the PJM is relatively small) and by much less than that in the other two muscles. However, from the point of view of a quantal packet of acetylcholine (ACh) traversing across the primary cleft to interact with the ACh receptor (AChR) at the PJM, the difference in AChe site density between the situation in which the distribution of AChe is only in the basal lamina along the PJM and the one in which the AChe is also in the lamina along the axonal membrane is a factor of 2. We do not know whether this "double layer" distribution of AChe in the primary cleft is also true for the neuromuscular junction of other muscles. Recently, Vigny et al. (46) suggested that the endplate-specific AChe in sternomastoid muscle is restricted to the postjunctional membrane. Until this matter is resolved, we cannot draw any definitive conclusions as to whether the additional layer of AChe in the primary cleft of the extraocular muscle has any significance in connection with the higher speed of this muscle, although this is a tempting speculation (18).

Recent studies have shown that the AChR is concentrated at 25,000–30,000 sites/μm^2 on a morphologically specialized thickened region on the top of the PJM in several mouse muscles (16, 17, 29). This has altered our thinking about the neuromuscular junction and has modified previous kinetic calculations (38) which had been based on the assumption of the mosaic model of Barnard et al. (2) which stated that the AChR is uniformly distributed down the postjunctional folds as is the AChe. Preliminary studies from our laboratory now also suggest that in the extraocular muscle of the mouse there is again a high concentration of AChR at the top of the postjunctional folds, as we had previously reported for the sternomastoid muscle (17). The AChe is thus present over the receptive surface at a 5- to 10-fold lower site density than is the AChR. Based on this molecular organization, a model of neuromuscular function has been proposed (17, 26) which suggests that each quantum of ACh interacts with a small postjunctional area at saturating local ACh concentration. For a quantum packet of 10^4 molecules (25), this area would be about 0.3 μm^2. The ratio of AChe to AChR in this region may become critical in controlling the speed of recovery after the ACh has interacted with receptor. It appears that in its basic form this model may also apply to the extraocular muscle. It is therefore of particular interest to determine whether the "double layer" of AChe in the primary cleft is unique to the fast muscle and what its significance is.

We thank Julie Matthews-Bellinger and Howard Howland for their useful discussions and Nikki Wolfe for her dedicated technical assistance.

This work was supported by National Institute of Neurological Disease and Stroke grant NS-09315.

Published previously in preliminary form (42)

Received for publication 21 December 1977, and in revised form 21 March 1978.

REFERENCES

1. Bach y Rita, P., and F. Ito. 1966. In vivo studies on fast and slow muscle fibers in cat extraocular muscles. *J. Gen. Physiol.* **49**:1177–1198.
2. Barnard, E. A., T. H. Chiu, J. Jedrzejcyzk, C. W. Porter, and J. Wieckowski. 1973. Acetylcholine receptor and cholinesterase molecules of vertebrate skeletal muscles and their nerve junctions. *In* Drug Receptors. H. P. Rang, editor. Macmillan, Inc., New York. 225–240.
3. Barnard, E. A., and A. W. Rogers. 1967. Determination of the number, distribution and some *in situ* properties of cholinesterase molecules in the motor endplates, using labeled inhibitor methods. *Ann. N. Y. Acad. Sci.* **144:** 584–594.
4. Barnard, E. A., T. Rymaszewska, and J. Wieckowski. 1971. Cholinesterases at individual neuromuscular junctions. *In* Cholinergic Ligand Interactions. D. J. Triggle, J. F. Moran, and E. A. Barnard, editors. Academic Press, Inc., New York. 175–197.
5. Berends, F., C. H. Postumus, I. V. D. Sluys, and F. A. Deierkauf. 1959. The chemical basis of the ageing process of DFP-inhibited pseudocholinesterase. *Biochim. Biophys. Acta.* **34**:576–578.
6. Betz, W., and B. Sakmann. 1971. "Disjunction" of frog neuromuscular synapses by treatment with proteolytic enzymes. *Nat. New Biol.* **232**:94–95.
7. Betz, W., and B. Sakmann. 1973. Effects of proteolytic enzymes on function and structure of frog neuromuscular junctions. *J. Physiol. (Lond.).* **230**:673–688.
8. Brown, G. L., and A. M. Harvey. 1941. Neuromuscular transmission in the extrinsic muscle of the eye. *J. Physiol. (Lond.).* **99**:379–399.
9. Cohen, J. A., R. A. Oosterbaan, H. S. Jansz, and F. Berends. 1959. The active site of esterases. *J. Cell. Comp. Physiol.* **54**:231–244.
10. Cooper, S., and J. C. Eccles. 1930. The isometric responses of mammalian muscles. *J. Physiol. (Lond.).* **69**:377–385.
11. Coult, D. B., D. F. Marsh, and G. Read. 1966. Dealkylation studies on inhibited acetylcholinesterase. *Biochem. J.* **98**:869–873.

12. COUTEAUX, R. 1972. Structure and cytochemical characteristics of the neuromuscular junction. International Encyclopedia of Pharmacology and Therapeutics. Pergamon Press, Inc., New York. **1**:7-56.
13. CSILLIK, B. 1965. Functional Structure of the Postsynaptic Membrane in the Myoneural Junction. Akademiai Kiado, Budapest, Hungary. 113-129.
14. DAVIES, D. F., and A. L. GREEN. 1956. The kinetics of reactivation by oximes of cholinesterase inhibited by organophosphorus compounds. *Biochem. J.* **63**:529-535.
15. DAVIS, R., and G. B. KOELLE. 1967. Electron microscopic localization of acetylcholinesterase and nonspecific cholinesterase at the neuromuscular junction by gold thiocholine and gold-theolactic acid methods. *J. Cell Biol.* **34**:157-171.
16. FERTUCK, H. C., and M. M. SALPETER. 1974. Localization of acetylcholine receptor by ^{125}I-labeled α-bungarotoxin binding at mouse motor endplates. *Proc. Natl. Acad. Sci. U.S.A.* **71**:1376-1378.
17. FERTUCK, H. C., and M. M. SALPETER. 1976. Quantitation of junctional and extrajunctional acetylcholine receptors by electron microscope autoradiography after ^{125}I-α-bungarotoxin binding at mouse neuromuscular junctions. *J. Cell. Biol.* **69**:144-158.
18. GAINER, H., and J. E. KLANCHER. 1965. Neuromuscular junctions in a fast contracting fish muscle. *Comp. Biochem. Physiol.* **15**:159-165.
19. HALL, Z., and R. B. KELLY. 1971. Enzymatic detachment of endplate acetylcholinesterase from muscle. *Nat. New Biol.* **232**:62-63.
20. HESS, A., and G. PILAR. 1963. Slow fibers in the extraocular muscles of the cat. *J. Physiol. (Lond.).* **169**:780-798.
21. HOBBINGER, F., 1956. Chemical reactivation of phosphorylated human and bovine true cholinesterase. *Br. J. Pharmacol.* **11**:295-303.
22. HOLMES, R., and E. L. ROBINS. 1955. The reversal by oximes of neuromuscular block produced by anticholinesterases. *Br. J. Pharmacol.* **10**:490-495.
23. JANSZ, H. S., D. BRONS, and M. G. P. WARRINGA. 1959. Chemical nature of the DFP binding site of pseudocholinesterases. *Biochim. Biophys. Acta.* **34**:573-575.
24. KARNOVSKY, M. J., and L. ROOTS. 1964. A "direct-coloring" thiocholine method for cholinesterase. *J. Histochem. Cytochem.* **12**:219-221.
25. KUFFLER, S., and D. YOSHIKAMI. 1975. Number of transmitter molecules in a quantum: an estimate from iontophoretic application of acetylcholine at the vertebrate neuromuscular synapse. *J. Physiol. (Lond.).* **251**:465-482.
26. MATTHEWS-BELLINGER, J., and M. M. SALPETER. 1978. Distribution of acetylcholine receptors at frog neuromuscular junctions with a discussion of physiological implications. *J. Physiol. (Lond.).* In press.
27. MCLEAN, I. W., and P. K. NAKANE. 1974. Periodate-lysine-paraformaldehyde fixative; a new fixative for immunoelectron microscopy. *J. Histochem. Cytochem.* **22**:1077-1983.
28. MCMAHAN, U. J., J. R. SANES, and Y. M. MARSHALL. 1978. Cholinesterase is associated with the basal lamina at the neuromuscular junction. *Nature (Lond.).* **271**:172-174.
29. PORTER, C. E., and E. A. BARNARD. 1975. The density of cholinergic receptors at the endplate post synaptic membrane; ultrastructural studies in two mammalian species. *J. Membr. Biol.* **20**:31-49.
30. ROGERS, A. W. 1973. Techniques of Autoradiography. Elsevier North-Holland, Inc., New York. 313-328.
31. ROGERS, A. W., A. DARZYNKIEWICZ, E. A. BARNARD, and M. M. SALPETER. 1966. Number and location of acetylcholinesterase molecules at motor endplates of the mouse. *Nature (Lond.).* **210**:1003-1006.
32. ROGERS, A. W., Z. DARZYNKIEWICZ, K. OSTROWSKI, M. M. SALPETER, and E. A. BARNARD. 1969. Quantitative studies on enzymes in structures in striated muscles by labeled inhibitor methods. I. The number of acetylcholinesterase molecules and of DFP-reactive sites at motor endplates measured by radioautography. *J. Cell Biol.* **41**:665-685.
33. SALPETER, M. M. 1967. Electron microscope radioautography as a quantitative tool in enzyme cytochemistry. I. The distribution of acetylcholinesterase at motor endplates of vertebrate twitch muscle. *J. Cell Biol.* **32**:379-389.
34. SALPETER, M. M. 1969. Electron microscope radioautography as a quantitative tool in enzyme cytochemistry. II. The distribution of DFP-reactive sites at motor endplates of a vertebrate twitch muscle. *J. Cell Biol.* **42**:122-134.
35. SALPETER, M. M., and L. BACHMANN. 1964. Autoradiography with the electron microscope. *J. Cell Biol.* **22**:469-477.
36. SALPETER, M. M., and L. BACHMANN. 1972. Autoradiography. *In* Principles and Techniques of Electron Microscopy, Biological Applications. M. A. Hayat, editor. Van Nostrand Reinhold Co., New York. **2**:221-278.
37. SALPETER, M. M., L. BACHMANN, and E. E. SALPETER. 1969. Resolution in EM radioautography. *J. Cell Biol.* **41**:1-20.
38. SALPETER, M. M., and M. E. ELDEFRAWI. 1973. Sizes of endplate compartments, densities of acetylcholine receptor, and other quantitative aspects of neuromuscular transmission. *J. Histochem. Cytochem.* **21**:769-778.
39. SALPETER, M. M., and F. A. MCHENRY. 1973. Electron microscope autoradiography: analysis of autoradiograms. *In* Advanced Techniques in Biological Electron Microscopy. J. K. Koehler, editor. Springer-Verlag, Berlin. 133-152.

40. SALPETER, M. M., F. A. McHENRY, and H. FENG. 1974. Myoneural junctions in the extraocular muscles of the mouse. *Anat. Rec.* **179:**201-224.
41. SALPETER, M. M., H. PLATTNER, and A. W. ROGERS. 1972. Quantitative assay of esterases in endplates of mouse diaphragm by electron microscope autoradiogrpahy. *J. Histochem. Cytochem.* **20:**1059-1068.
42. SALPETER, M. M., and A. W. ROGERS. 1971. Pre- and postjunctional localization of acetylcholinesterase by quantitative EM autoradiography. 1st Annual Meeting for the Society for Neurosciences. 118 (Abstr.)
43. SALPETER, M. M., and M. SZABO. 1972. Sensitivity in electron microscope autoradiography. I. The effect of radiation dose. *J. Histochem. Cytochem.* **20:**425-434.
44. WILSON, I. B., S. GINSBURG, and C. QUAN. 1958. Molecular complimentariness as basis for reactivation of alkyl phosphate inhibited enzyme. *Arch. Biochem. Biophys.* **77:**286-296.
45. WILSON, I. B., and H. C. FROEDE. 1971. The design of reactivators for irreversibly blocked acetylcholinesterase. *In* Drug Design. E. J. Ariens, editor. Academic Press, Inc., New York. **2:**213-229.
46. VIGNY, M., J. KOENIG, and F. REIGER. 1976. The motor endplate specific form of acetylcholinesterase appearance during embryogenesis and reinnervation of rat muscle. *J. Neurochem.* **27:**1347-1352.